Is there Need of any Modulation in the Pyramid Wavefront Sensor?

Joana Buechler Costa[a], Roberto Ragazzoni[a,c], Adriano Ghedina[b],
Marcel Carbillet[c], Christophe Verinaud[c], Markus Feldt[a],
Simone Esposito[c], Elena Puga[a] and Jacopo Farinato[c]

[a]Max-Planck-Institut für Astronomie (MPIA), Königstuhl 17, Heidelberg 69117, Germany
[b]Telescopio Nazionale Galileo, La Palma, Spain
[c]Astronomical Observatory of Arcetri, Firenze, Italy

ABSTRACT

In the pyramid wavefront sensor some dynamic range is accomplished by modulating the optical signal across the four faces of the pyramid before the dissection and detection of the light. Although this can be realized in different ways, including systems which do not require any moving part, we question and discuss the real needs for such a modulation. In fact, when the closed-loop performance is not perfect, some residual errors on the wavefront sensor are expected and one should take care to allow for enough dynamic range to get a linear response within such a residual range. However, the non-corrected aberrations themselves can be considered as a form of modulation. Higher order uncompensated residuals are equivalent to a modulation for the lower compensated modes.
We present a preliminary study showing that this sort of 'natural' modulation could be, at least under certain conditions, enough to reach comparable results with respect to dynamical modulation during correction, hence rising the question of the need of a modulation in the realization of the pyramid wavefront sensor.

Keywords: Pyramid wavefront sensor, modulation

1. INTRODUCTION - WHY NOT MODULATE?

In the optical geometrical approximation the modulation of a Pyramid Wavefront Sensor (PWFS in the following) plays a central role as it dictates the equivalent focal length of the lenslet array of the Shack–Hartmann wavefront sensor having the same characteristics, at least if the latter is used with a four–quadrant mode to detect the position of the various spots. No modulation translates into infinite focal length and, even in geometrical approximation, this simply means that the signal of the PWFS saturates as soon as the first derivative of the wavefront would not be strictly flat. In other words the PWFS would be able just to give the sign of the derivative of the wavefront and not any estimation of its amplitude, because, in geometrical approximation, the light spot can be arbitrarily small. Modulation ensures a certain dynamic range prior to the saturation of the signal. In real–world of course spot size is not arbitrarily small and, by heuristic reasoning, it has been shown that sensitivity of a PWFS without any modulation is significantly larger than for the Shack–Hartmann sensor.[1] Because of the small dynamic range, however, whenever the residual aberrations as seen on the PWFS are larger than the dynamic range, some non–linearity will occur leading to a deterioration of the performance. This interesting feature has been studied[2] and it has been shown that, at least under the conditions simulated in the related work, it does usually exist a best modulation amplitude making the magnitude gain the largest as possible.

While we do not investigate here the effects of non–common path aberrations that can lead to a use of modulation to simply avoid to use the wavefront sensor in its saturated regime, regardless of the above–mentioned consideration, it is to be pointed out that there are some reasons to raise the question if a PWFS without

Further author information: (Send correspondence to J.B.C.)
J.B.C.: E-mail: costa@mpia.de, Telephone: +49 6221 528335

Adaptive Optical System Technologies II, Peter L. Wizinowich, Domenico Bonaccini,
Editors, Proceedings of SPIE Vol. 4839 (2003) © 2003 SPIE · 0277-786X/03/$15.00

modulation can still work at its best conditions, even with a residual aberration different from zero, or, at least, with a small lack of performance. As the absence of modulation is of course a large simplification of the PWFS optical design, especially for the multi–WFS conceived for MCAO, this is for sure an interesting topic.

Modulation can be seen as the superposition of a tilt made in an *incoherent* way making the spot larger than its original size. The incoherence here is attained by temporal averaging and for this reason, the spot still preserves all the wavefront information. A different technique described elsewhere[3] uses a coherent modulation by introducing some high order spatial frequencies. These are to be selected in a way to enlarge the spot size but, simultaneously, to avoid to introduce perturbation on the modes that one wants to measure. In other words the content of low spatial frequency should be closely enough to zero so as not to perturb the measurement.

The key point is that residual aberration can play such a role in a *natural* way. It is clear, from the above reasoning, that to avoid saturation and hence non–linearity effects one would need modulation proportional to the amount of residual aberrations in closed loop. On the other hands the residual aberrations are, by definition, proportional to the residuals. Not all the residuals are useful, however. We can distinguish phenomenologically the following two:

1. Aberrations at spatial frequencies larger than the ones sensed by the PWFS. These automatically can play the role of *natural* modulation and their strengthness is dictated by the number of corrected modes and by the spectrum of turbulence;
2. Aberrations sensed by the wavefront sensor and only partially corrected. In this case still these can play the role of natural modulation, but limited to the modes of lower spatial frequencies.

To make a practical examples, for a system performing Adaptive Optics (AO) up to Z50, the mode Z80 characterizes the first category and can play some role in the modulation of all the sensed modes, while the mode Z30 can be useful to modulation for the sensing of the modes smaller than this only.

All these considerations alone are not, of course, enough to establish firmly if modulation can be avoided at all (on the other hand it can be easily seen that by building a turbulence spectrum *ad–hoc* there is clearly need of modulation in a number of occasions) but provides some physical means on which basis a similar results can be founded. Although not exhaustive, we list in the following various analytical, numerical, and on–sky experimental examples where no modulation during correction gives at least comparable results with respect to dynamical modulation.

2. GENERAL

The principle of the PFWS has been well described in many other papers so that we just refer the conclusions important to this work.[4–6] With a pyramid wavefront sensor the local wavefront slope at (x, y) in the entrance pupil is calculated by the following procedure. First the signals S_x and S_y are determined which are calculated with the intensities at the conjugated points of (x, y) in the four pupils on the detector (x_p, y_p), according to:

$$S_x(x,y) = \frac{\Big(I_1(x_p,y_p) + I_4(x_p,y_p)\Big) - \Big(I_2(x_p,y_p) + I_3(x_p,y_p)\Big)}{\sum_{i=1}^{4} I_i(x_p,y_p)} \tag{1}$$

$$S_y(x,y) = \frac{\Big(I_1(x_p,y_p) + I_2(x_p,y_p)\Big) - \Big(I_3(x_p,y_p) + I_4(x_p,y_p)\Big)}{\sum_{i=1}^{4} I_i(x_p,y_p)} \tag{2}$$

In geometric optics regime this gives the local slope of the wavefront the point (x, y):

$$\frac{\partial W(x,y)}{\partial x} = \frac{A}{f}\left(\frac{\pi}{2} S_x\right) \tag{3}$$

where A is the modulation amplitude, f the focal length and W the wavefront in the entrance pupil. The y components are analogous. From this equations we can see that without modulation the signals on the wavefront sensor would be infinite. We could only detect the sign of the wavefront slope by detecting which of the 4 pupils is illuminated.
If we observe the situation with diffraction optics we have to work with the electric fields in the entrance, pyramid and detector plane. This means we have to take into account the diffraction effects at the pyramid edges. Using the approximation that we can describe the effect of a four-sided pyramid by 2 two-sided pyramids with the edges perpendicular to each other (we are here discarding the diffraction effect of the other edge when calculating the diffraction in one direction). The result we obtain for the signals is:

$$S_x(x_p, y_p) = \frac{[(I_1 + I_4) - (I_2 + I_3)]_{(x_p, y_p)}}{\sum_{i=1}^{4} I_i(x_p, y_p)} \tag{4}$$

$$\propto \int_{-B(y_p)}^{B(y_p)} \frac{\sin\left(\phi(x, y_p) - \phi(x_p, y_p)\right)}{(x - x_p)}\, dx \tag{5}$$

Here we have I_i being the intensity falling on the pixel corresponding to (x, y) on pupil i. The limits of integration are the borders of the pupil chord $y = y_p$. The S_y is of course analagous. This has been deduced elsewhere.[5]

3. LINEARITY

We see from eq.5 that the signal at point (x_p, y_p) is proportional to the integration of the sinus of the phase difference between each point on the chord $y = y_p$ (which is perpendicular to the vertex), weighted according to his distance between both points. More distant points, with a higher probability of differing more in phase, will be weighted less.
Looking only at the sinus we have a linear relation between the intensity distribution on the pupil images and the phase differences in the entrance pupil if:

$$\sin\left(\phi(x, y_p) - \phi(x_p, y_p)\right) \cong \phi(x, y_p) - \phi(x_p, y_p) \tag{6}$$

Using Taylor:

$$\sin(x) = x - \frac{x^3}{3!} + \frac{x^5}{5!} + \ldots \tag{7}$$

To have $\sin x \cong x$, the x^3-Term has to be small compared to x. This means, f.ex.:

$$| x | > 10\frac{| x^3 |}{3!} \quad \Rightarrow \quad | x | < \sqrt{\frac{6}{10}} \tag{8}$$

or generally: (9)

$$| x | > 10^k\frac{| x^3 |}{3!} \quad \Rightarrow \quad | x | < \sqrt{\frac{6}{10^k}} \tag{10}$$

if we want the second term to be k orders smaller.
Now we can calculate for each Zernike-aberration the Peak-to-Valley value depending on it's coefficient. Then we can restringe it according to eq.10 and we obtain a value for the maximum aberration coefficient. As an example, for spherical aberration[7]:

$$\phi(\rho, \theta) = 1/\sqrt{2}\, A_{040}\, (6\rho^4 - 6\rho^2 + 1) \tag{11}$$

$$\phi'(\rho, \theta) = 1/\sqrt{2}\, A_{040}\, (24\rho^3 - 12\rho) \tag{12}$$

this gives:

$$PV = \frac{9\, A_{040}}{8\sqrt{2}} \tag{13}$$

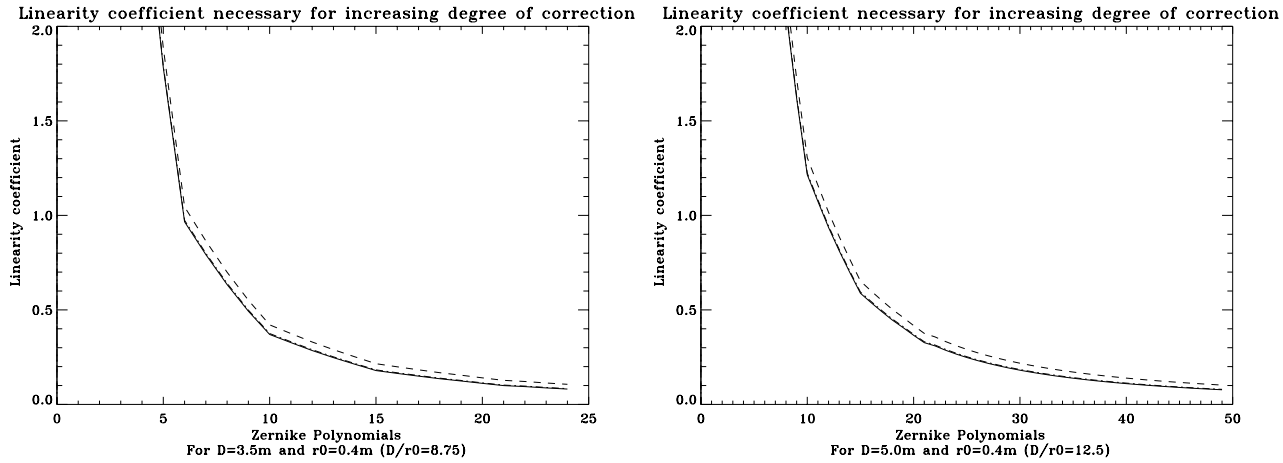

Figure 1. Number of Zernike Polynomials (Noll) that need to be corrected (in x-axis) to obtain a linear response from the sensor (definition of linearity in y-axis), for a ratio $D/r_0 = 8.75$ and 12.5. Dashed line means there is a residual of 10 % in each corrected mode. Almost superimposed to the continuous line there is the line–dot curve, which uses a residual of 1 % in each corrected mode.

This can now be substituted into eq. 10, giving:

$$k = 1 \quad \Rightarrow \quad \mid A_{040} \mid < 0.97 \tag{14}$$

$$k = 2 \quad \Rightarrow \quad \mid A_{040} \mid < 0.31 \tag{15}$$

This can be determined for all zernike polynomes, but maybe it is possible to use the RMS instead, which can be calculated for every polynom with:

$$(\Delta\phi)^2 = \overline{\phi^2} - \overline{\phi}^2 \tag{16}$$

$$= \frac{1}{2} \sum_{n=1}^{\infty} \sum_{m=0}^{n} \frac{{A_{nm}}^2}{n+1} \tag{17}$$

Using this we obtain of course a higher estimation of the maximum aberration coefficient value, in this case:

$$k = 1 \quad \Rightarrow \quad \mid A_{040} \mid < 2.45 \tag{18}$$

$$k = 2 \quad \Rightarrow \quad \mid A_{040} \mid < 0.77 \tag{19}$$

If we have a combination of different aberrations we have the total RMS beeing the sum of the RMS of each of them according to eq.17.
The Zernike polynomials permit an analytic evaluation of the residual wavefront errors after the first J modes are corrected[8,9]:

$$\Delta_J \approx 0.2944\, J^{-\sqrt{3}/2}\, (D/r_0)^{5/3}\ [rad^2] \tag{20}$$

$$\text{for} J > 10 \tag{21}$$

With this we can estimate when our response is going to be linear (according to a given linearity definition), depending on the degree of correction, the Fried parameter and the telescope diameter (see Fig.1). The linearity is defined by a linearity coefficient, given by the ratio of the second and the first terms in the expansion: $\frac{x^3/3!}{x}$. We have also plotted the curve when there is always 1/10 of the magnitude of the modes left after correction.

In Fig.2 we have plotted the $sin(x)$, x, and $sin(x) - x$. We see from this graph that when we approximate $sin(x)$ by x we have a quiet good estimate till $x \approx \pi/2$. After that, till $x \approx \pi(3.14\, rad)$ we still have an estimate that gives us the correct sign. This means, the best correction estimated like this will not be correct but it will be a correction in the right direction. Maybe overestimated (if the gain is set to 0), but in the next correction loops the aberration will decrease continuously.

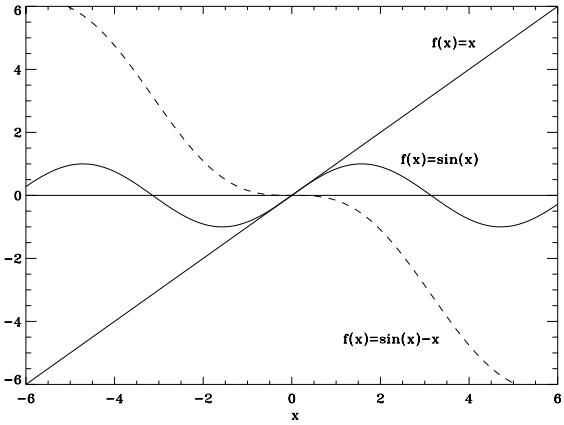

Figure 2. Plot of $sin(x)$ and x to visualise the linear domain.

4. INCREASING THE LINEARITY

Taking eq.5 we can write the phase in the entrance pupil as the sum of the phase due to high order aberrations, ϕ_H, and the phase due to low order aberrations, ϕ_L:

$$\phi = \phi_L + \phi_H \tag{22}$$

Accordingly, and referring only to the x variable, we can rewrite $sin(\phi(x) - \phi(x_p))$ as

$$\begin{aligned} \sin(\phi(x) - \phi(x_p)) &= \sin(\phi_L(x) - \phi_L(x_p)) \cos(\phi_H(x) - \phi_H(x_p)) & (23) \\ &+ \sin(\phi_H(x) - \phi_H(x_p)) \cos(\phi_L(x) - \phi_L(x_p)) & (24) \end{aligned}$$

This expression, divided by $x - x_p$ is going to be integrated along a chord ($y = y_p$). Analysing the first line we see that, as $\phi_H(x) - \phi_H(x_p)$ is varying at high frequency, it has the effect of erasing the contribution of $sin(\phi_L(x) - \phi_L(x_p))$, unless x is near x_p. In this case, since $sin(\phi_L(x) - \phi_L(x_p)/(x - x_p)$ can get very large, its contribution to the integral will be decreased by the effect of the *cos* but it will not be zero. Here we see that the high order frequencies have an effect that can be compared to a modulation, in the sense that they tend to act as a delta-function $\delta(x - x_p)$ in the integral, linearising the system. The higher the frequency or the higher the magnitude of the high orders, the larger is going to be this linearising effect. But since it decreases the integral contribution at the origin it will be accompanied by a loss in signal magnitude. This idea is ilustrated by numerical simulations in the following section (see also Fig.3).

5. SIMULATIONS

We have made a computer simulation of the Pyramid Wavefront System. The program follows the scheme:
On a circular entrance pupil we generate a matrix with the distribution of phases, the wavefront, that can be a surface described by Zernike polynomes or an arbitrary distribution of heights. The matrices used all had 512×512 points, where the imbedded pupil had a diameter of 128 points. The corresponding pupil function of this wavefront is Fourier-transformed. This gives us the E-Field in the focal plane, from which we can get the Point Spread Function (PSF). This E-Field is now subjected to phase shifts corresponding to the phase shifts that a glass pyramid with a certain refraction index and geometry would provoke.
Through a second Fourier-transform we get the E-field in the pupil image plane. We can now calculate the intensity in the pupil image plane. We obtain 4 pupils, and each of them is binned into a given number of pixels (corresponding to the detector pixels, in our case 16 per diameter). With this we can calculate the signal for each pupil image pixel.
This simulation allows us to calculate the interaction matrix of the system. The interaction matrices for all the

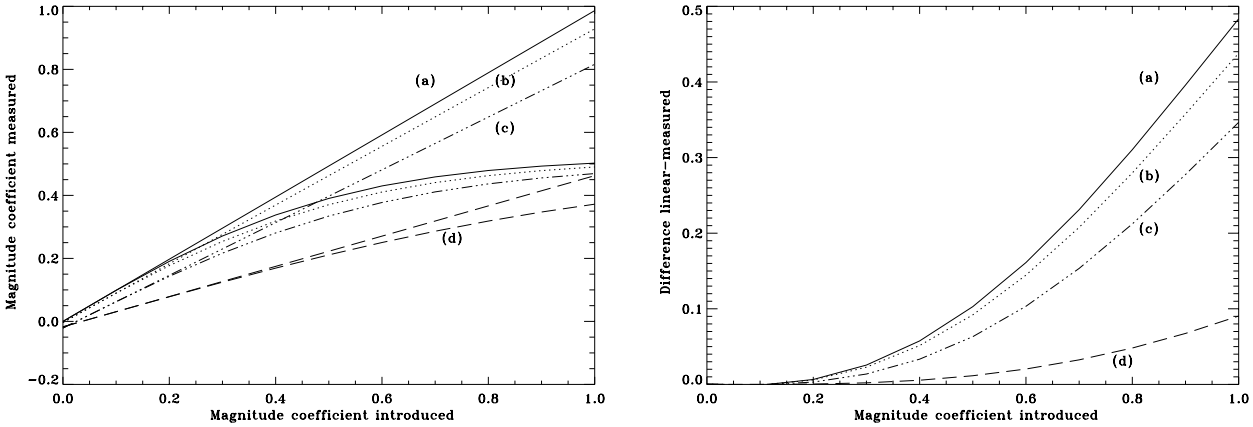

Figure 3. left: Magnitude of measured coefficient of $z4$ (defocus) for different introduced coefficient magnitudes (units described in the text). The continuous line represents a measurement without higher order residuals. The other ones represent the measurement done with higher order residuals (for description in detail see the text). For each curve there is also plotted a linear fit tangent to the origin. The higher order residuals correspond to $r0 = 0.6\,m$ and for a telescope diameter of $5.7\,m$.
right: Difference between linear fit and measurement curve.
For explanation see text.

simulations were done for 36 Zernike polynomials, but always with a very small magnitude, so that we were for sure estimating them in the linear regime. Through SVD we get the reconstruction matrix and the singular values.
There is also the possibility to use the simulation with modulation. This means, we rotate the "focus" on the pyramid around the edge and integrate the intensities obtained on the pupil image plane. As before we can get the interaction matrix, reconstruction matrix and singular values also for this case.

We have done simulations of measurements and compensations in open-loop and closed-loop.

With the simulation of measurements we can determine how the PFWS measures a given single aberration or pattern. In Fig.3 we plotted the measured magnitude of coefficient $z(4)$ against the introduced one. The units are chosen in a way that, with a wavefront with an aberration of 1.0 of a certain coefficient originates a phase distribution with standard deviation of 1 rad. The reconstruction matrix used was made for coefficient magnitudes of 0.0081, so that it was taken in perfectly linear regime. The continuous curve (a) are the results obtained from increasing defocus magnitude. The broken lines represent the same simulation but introducing high order frequencies.
We have[9]

$$\Delta_J = \langle \phi^2 \rangle - \sum_{j=1}^{J} \langle |a_j|^2 \rangle \tag{25}$$

where $\langle \phi^2 \rangle$ is the phase variance, a_j the coefficient of mode J and Δ_J the mean square residual error after correcting all the modes till J. From this we get

$$\Delta_J - \Delta_{J+1} = \langle |a_{J+1}|^2 \rangle \tag{26}$$

or using the Noll's approximated formula

$$\langle |a_{J+1}|^2 \rangle \approx 0.2944 \left(\frac{D}{r_0}\right)^{\frac{5}{3}} \frac{\sqrt{3}}{2} J^{-1-\frac{\sqrt{3}}{2}}, \text{for } J > 10 \tag{27}$$

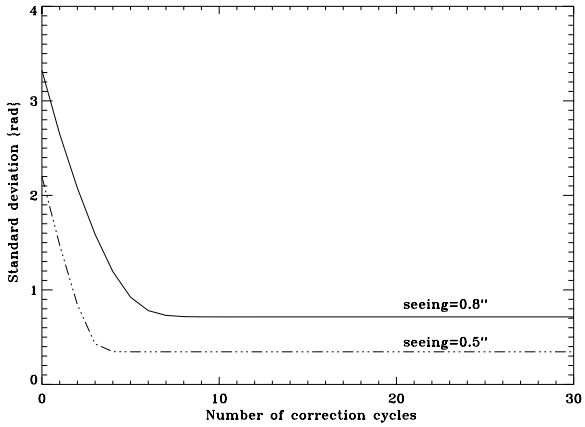

Figure 4. Evolution of the standard deviation of corrected phasescreens with different initial parameters as a function of the number of correction cycles.

We can now calculate the magnitude of each coefficient for given telescope diameter and r_0.

The dotted line (b) represents the magnitude of the measured coefficients when the residual consists in 1/10 of the Noll magnitude for all the polynoms with higher frequency than $z4$ till $z36$. For the dashed line (d) we used as a residual 1/10 of the Noll magnitude for all the orders bigger than $z4$ till $z36$ and included the complete magnitude (given in eq.27) from the orders $z37$ till $z45$. For the line–3dots curve we used as residual as before 1/10 of the Noll magnitude for all the orders bigger than $z4$ till $z28$ and included the complete magnitude from the orders $z29$ till $z36$. By tracing a straight line tangent to each of the curves at the origin and measuring the deviation from the straight lines to the curves (see Fig.3 on the right side) we can see that the deviation from linearity in the dotted lines is smaller than in the continuous line, beeing the behaviour more linear when we use as residual the natural magnitude (without partial compensation) of higher orders. The same lines can be used for different parameters D or r_0. With the linear fit we can estimate the gain that should be used to achieve the best results. We have done this also for some other zernike polynoms and it seems that the estimated gain is more or less constant.

Open-loop compensation means that we have introduced an aberrated wavefront into the system, reconstructed it and calculated the best correction. This can be done in more than one step depending on how the improve-

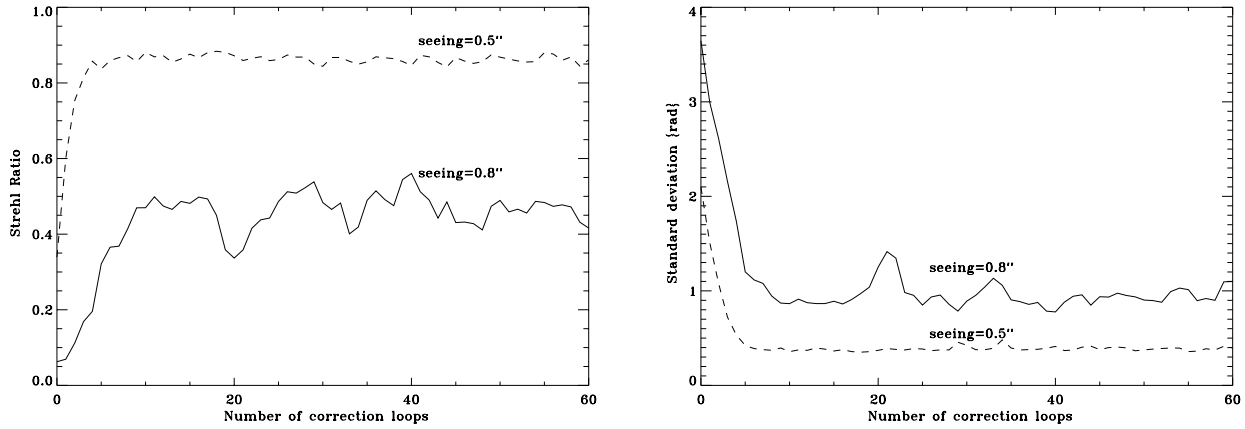

Figure 5. Evolution of the Strehl Ratio and the standard deviation for different atmospheric conditions in closed loop compensation.

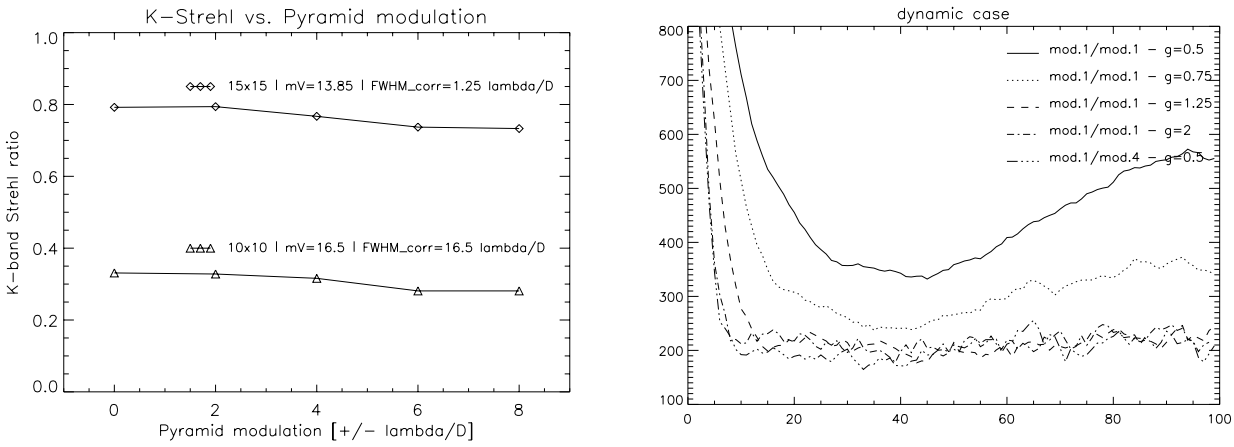

Figure 6. left: Strehl ratios achieved in K-band for closed-loop compensation with different modulation amplitudes. In the top curve we have a good SNR (mV=13.85), while in the bottom one we have a poor SNR (mV=16.5).
right: Wavefront deviation (in arbitrary units) as a function of the increasing loop step number for different combinations of calibration and correction modulations.

ment is developing. This does not take into account a temporal change of the wavefront. As input we have introduced generated phasescreens with different parameters (see Fig.4). These phasescreens were generated with the IDL code of TurbuLenZ,[10] a atmospheric turbulence simulator. Instead of a full-scale AO simulation, we smoothed the phase screens to a desired RMS to achieve the specific Strehl ratios.
For the closed-loop regime we have used a sequence of phasescreens that simulate the atmosphere at a rate of 1 screen per ms. This phasescreens have also been generated with TurboLenZ. We used 10 successive screens and integrated the intensity in the pupil images. From this integrated image we calculated the signals and reconstructed the wavefront. This, beeing the estimate of the wavefront, was subtracted from the following 10 screens and a new estimate (for the residual wavefront) was determined.
This was done for almost three seconds, that means for 300 correction cycles for a seeing of $0.5''$ and for 63 correction cycles with a seeing of $0.8''$. The parameters of the phasescreens are a τ_0 of $100\,ms$, a telescope diameter of $5.7\,m$ and a wavelength of $2.2\,\mu m$. The results in terms of residual standard deviation and Strehl ratio (SR) are shown in Fig.5. This plots include the bootstrapping phase. It can be seen from this simulation that it is possible to close the loop without modulation. Also during the experimental verification the system had no problems in bootstrapping (see sect.6).
Preliminary results from independent simulations, made for the first-light AO system of LBT[11] with a code (the software package CAOS) that permits the simulation of a dynamical modulation, have been used for comparing different cases with and without modulation. In Fig.6 on the left side there are two cases plotted, one with a good SNR (top) and the other one with a poor (bottom). The interaction matrices have been recorded with $\pm 7\lambda/D$ for the top and $\pm 8\lambda/D$ for the bottom curve. During the closed-loop there were used different modulations. The curves show that, when using an interaction matrix recorded with a given (relatively high) modulation, the differences between modulating or not during correction is small.

In the right plot, which is to be compared to the upper case of the left plot, we tried to use the same modulation that was used during calibration, $\pm 1\lambda/D$, also for the correction, only changing the gain. The result is that the performances could reach again the performance of the top curve in the left plot. All the curves should be compared to the 3dot-line, which represents correction at modulation $\pm 1\lambda/D$ and interaction matrix taken at $\pm 4\lambda/D$, with a gain of 0.5. These parameters allow the best average SR in this case (SR=0.767). Then the same simulation has been run with a modulation of $\pm 1\lambda/D$ during calibration. With a gain of 0.5 the performance is bad, because the temporal error is high. But for a gain of 1.25 the SR reaches 0.750, very near to the first case. This curve essentially shows that by optimising the gain of the loop, we retrieve, even with a

	Star Name	mV	Date	Time(UT)
1	HR3951	5.4	27/04/02	21:42
2	HR4550	6.1	27/04/02	22:35
3	HR5415	6.4	27/04/02	00:50
4	HR5280	7.1	27/04/02	01:38
5	HR5414	7.6	27/04/02	02:01
6	HD149662	7.4	27/06/02	23:09
7	HD149561	8.4	27/06/02	23:35
8	HD149579	9.2	28/06/02	01:29

Table 1. Stars observed for the test of the Pyramid Wavefront Sensor

matrix recorded at low modulation, the same result as by recording at high modulation and correcting at low modulation.
The comparisons presented in this section are far from being conclusive, and suggest a deeper analysis of the problem in order to properly disentangle the effects of loop gain, diffraction, and photon noise.

6. EXPERIMENTAL VERIFICATION WITH REAL STARS

The experimental verification was performed on sky with the PWFS of the Telescopio Nazionale Galileo (TNG), a 4m class telescope sited at the observatory of Roque de Los Muchachos, La Palma, Canary Islands. The adaptive optics module of TNG, AdOpt@TNG, is the only AO system that currently implements a pyramid as a WFS for AO, and its latest performances show that this kind of sensor is comparable to the WFS normally mounted on other AO systems.[12]

We choosed for the purposes of our test a set of 8 stars with scaling magnitudes from 5.4 to 9.2 and for each of them we took a serie of closed loop images, alternatively switching off and on the modulation of the pyramid. The pyramid of AdOpt@TNG is mounted on an XY stage, and to introduce or not the modulation is an immediate task. In this way the elapsed time between the two different measurements (with and without modulation) on the same star was negligible: this assures the same overall conditions of the system during the test.

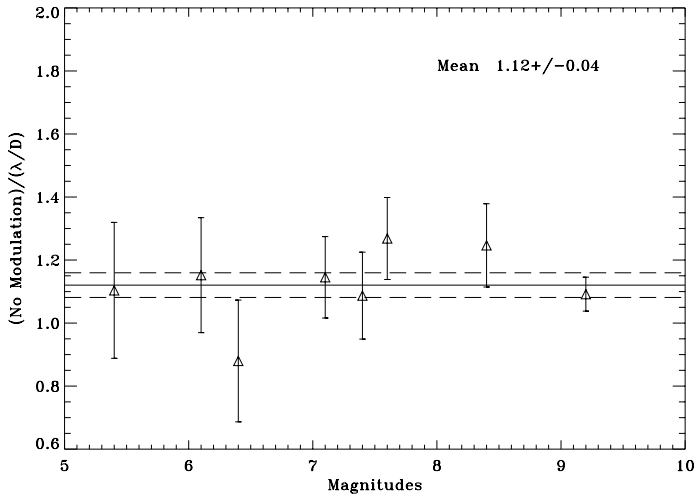

Figure 7. Ratio of S for no modulation (PWFS) versus λ/D modulation. Mean value is $\approx 1.12 \pm 0.04$.

On the pin of the pyramid at the plate scale of AdOpt@TNG, being the effective F ratio $F/32$, and at the effective wavelenght of sensing ($\lambda = 800$nm), the modulations of $\pm\lambda/D$ corresponds to a circular modulation with diameter $\approx 51\mu$m. Amplitude and frequency of the modulation where checked with an oscilloscope to correspond to the desired values.
Actually we splitted the pupil on the CCD into $\approx 8 \times 8$ subapertures, although correction was performed only up to the first 14 K–L polynomials. Accordingly to the number of corrected polynomials we could have sampled the pupil at 4×4 but we used the standard observational mode of AdOpt@TNG.
The differences in performance were calculated by direct Strehl measurements on the scientific cameras, and for every measurement we took several Strehl data with and without the modulation of the pyramid, but, as we said before, within a negligible amount of time between one measurement and the following.
To override in the analysis of the results some problems due to the change of the atmospheric and instrumental observing conditions we decided to explore only the ratio between the Strehls and not their absolute values, referring the no–modulation data to the data of the 51μm amplitude as it can be seen in Fig.7.
A fit of the experimental data of Fig.7 shows that the PWFS performs marginally better, being the mean value of the ratio 1.12 ± 0.04, when there is no dynamic modulation of the pyramid. Anyway we have to point out that, as described in the theory, the residual of the correction on the pin of the pyramid can be considered as a modulation itself, from which it seems straightforward that it is better to not modulate. However we have always been during the observations in the condition that the correction was not full but limited, that is far from the diffraction limit on the pin of the pyramid, a regime where maybe other diffraction effects could play an important role.

7. CONCLUSIONS

We discussed, with different approaches, various situations where a sensing of the wavefront can be done with no modulation. The situations studied point to the conclusion that using the PWFS without modulation and applying the correct gain, the loop can be closed. If this can happen without loss of the PWFS potential still needs to be confirmed. We studied the effect of the residuals left from partial correction, as well as the residuals generated by orders higher than the ones sensed by the sensor, as linearisation of the system.
At this stage of the study, we can say that we have enough hints for pursuing our investigations in order to determine if and when modulation is actually required. Some hints tend to show that, at least at low SNR, natural modulation seems to possibly overcome the need of an additional dynamic modulation. The answer to this question is very important indeed, since it determines the complexity of the optical design of the wavefront sensors, especially in the multi-reference scheme.

ACKNOWLEDGMENTS

J.B.C. wishes to thank Filipe Paccetti for all the helpful discussions and comments on this work. E.P. wishes to acknowledge the funding supported by the European Commission RTN program: "Adaptive Optics for Extremely Large Telescopes", under contract: HPRN-CT-2000-00147.

REFERENCES

1. R. Ragazzoni and J. Farinato, "Sensitivity of a pyramidic wave front sensor in closed loop adaptive optics," *A&A* **305**(L23-L26), 1999.
2. S. Esposito and A. Riccardi, "Pyramid wavefront sensor behavior in partial correction adaptive optic systems," *A&A* **369**(L9), 2001.
3. R. Ragazzoni, E. Diolaiti, and E. Viard, "A pyramid wavefront sensor with no dynamic modulation," *Opt. Comm* **208**(51), 2002.
4. R. Ragazzoni, "Pupil plane wavefront sensing with an oscillating prism," *J. Modern Opt.* **43**(2), pp. 289–293, 1996.

5. S. Esposito, A. Riccardi, and O. Feeney, "Closed-loop performance of pyramid wavefront sensor," in *Proc. SPIE Vol. 4034, p. 184-189, Laser Weapons Technology, Todd D. Steiner; Paul H. Merritt; Eds.*, **4034**, pp. 184–189, July 2000.
6. S. Esposito, O. Feeney, and A. Riccardi, "Laboratory test of a pyramid wavefront sensor," in *Proc. SPIE Vol. 4007, p. 416-422, Adaptive Optical Systems Technology, Peter L. Wizinowich; Ed.*, **4007**, pp. 416–422, July 2000.
7. M. Born and E. Wolf, *Principles of optics*, 1999.
8. D. L. Fried, "Statistics of a Geometric Representation of Wavefront Distortion," *J. Opt. Soc. Am.* **55**, pp. 1427–1435, 1965.
9. R. J. Noll, "Zernike polynomials and atmospheric turbulence," *J. Opt. Soc. Am.* **66**(3), 1976.
10. T. Berkefeld, R. Weiss, and A. Glindemann, "Simulations of kolmogorov phase screens - algorithms and applications," *submitted to Appl. Opt.* , 2002.
11. M. Carbillet, C. Verinaud, S. Esposito, A. Riccardi, A. Puglisi, B. Femenia, and L. Fini, "Performance of the first-light AO system of LBT by means of CAOS simulations," in *Adaptive Optical System Technologies II, this conference*, *Proc. SPIE* **4839**, Aug. 2002.
12. A. Ghedina, M. Cecconi, R. Ragazzoni, J. Farinato, A. Baruffolo, G. Crimi, E. Diolaiti, S. Esposito, L. Fini, M. Ghigo, E. Marchetti, T. Niero, and A. Puglisi, "On Sky Test of the Pyramid Wavefront Sensor," in *Adaptive Optical System Technologies II, this conference*, *Proc. SPIE* **4839**, Aug. 2002.